JACS
JOURNAL OF THE AMERICAN CHEMICAL SOCIETY
Article
pubs.acs.org/JACS

Versatile Strategy for Biochemical, Electrochemical and Immunoarray Detection of Protein Phosphorylations

Sanela Martić,[†] Michelle Gabriel,[‡] Jacob P. Turowec,[‡] David W. Litchfield,[‡,*] and Heinz-Bernhard Kraatz[†,*]

[†]Department of Physical and Environmental Sciences, University of Toronto Scarborough, Toronto, Ontario M1C 1A4, Canada, and Department of Chemistry, University of Toronto, Toronto, Ontario M5S 3H6, Canada

[‡]Department of Biochemistry, Schulich School of Medicine and Dentistry, Western University, London, Ontario N6A 5C1, Canada

Supporting Information

ABSTRACT: Protein kinases catalyze the phosphorylation of cellular proteins involved in the regulation of many cellular processes and have emerged as promising targets for the treatment of several diseases. Conventional assays to monitor protein kinase activity are limited because they typically rely on transfer of radioactive phosphate or phospho-specific antibodies that recognize specific substrates or sequence motifs. To overcome the limitations of conventional assays, we have developed a versatile approach based on transfer of ferrocene-phosphate that can be readily monitored using electrochemical detection or detection with antiferrocene antibodies in an immunoarray format. This assay is readily adapted to multiplex arrays and can be employed for monitoring kinase activity in complex mixtures and for kinase inhibitor profiling.

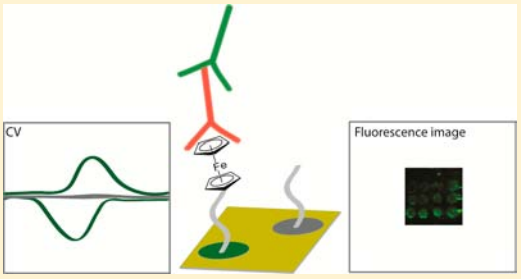

INTRODUCTION

Protein kinases catalyze the phosphorylation of proteins and modulate fundamental cellular function including cell regeneration and death.[1] Hyperactivity of some kinases is recognized as a molecular cause for diseases, including some cancers and tauopathies.[2] As a result, signal pathways involving protein kinases are currently undergoing intense study. The activity of protein kinases can be down-regulated with the help of small molecular inhibitors and as such are viewed as drugable targets for therapeutic applications.[3] Currently, the gold standard for monitoring protein kinase activities and inhibition is the a [γ-^{32}P]ATP radiometric assay,[4] and has been applied to the multiplexed detection of phosphorylations on peptide chips.[5] Radioactivity is an obvious drawback. An alternative to radiolabeling is an immunoassay approach using nonlabeled or fluorescently labeled antiphospho antibodies (phospho-Ab) for detection of specific phosphorylation products.[6] Currently, the phospho Ab are phosphorylation-site dependent (pSer/pThr/pTyr) and exhibit minimal cross reactivity with non-phosphorylated residues but are found to be promiscuous. In addition, phospho-Ab methodology is less compatible with a multiplexed array format and with high-throughput screening, which require multiple phospho-Ab for the detection of phosphorylation. Given a large kinome library which includes over 500 protein kinases and substrates, hundreds of phospho-Ab targets are currently commercially available whose epitopes target pSer/pThr/pTyr of a specific substrate, which helps in kinase profiling and identification. Toward developing new platforms for the protein kinase detection, a range of analytical methods based on phospho-Ab are available such as fluorescence,[7] surface plasmon resonance (SPR),[5a] electrochemical impedance spectroscopy,[8] quartz-crystal microbalance,[9] and magnetic resonance imaging.[10] Alternatively, a small phosphosensor molecule may be used in a peptide microarray format, which altogether eliminates the need for Ab chemistry.[11] Alternatives to immunoassays and/or radiolabeled assays are based on nanoparticles,[12] mass spectrometry,[13] electrochemistry,[14] and fluorescence,[15] and occasionally employ the use of γ-modified ATP cosubstrates.[16]

In an effort to develop an alternative to commonly used methodologies, we designed 5′-γ-ferrocenyl (Fc)-adenosine triphosphate (Fc-ATP) shown in Figure 1 and demonstrated its utility for the electrochemical detection of kinase-catalyzed phosphorylations of the surface-bound peptides.[14a] Such Fc-phosphorylated films on gold produced a quantifiable redox response that can be exploited for kinase activity profiling and inhibitor studies even under dirty conditions.

In this work, we present a methodology that is complementary to our electrochemical approach, making use of a robust polyclonal rabbit antiferrocene (Fc) antibody (Fc-Ab$_1$), which in combination with Fc-phosphoryl transfer represents a powerful new approach to monitoring protein kinases activity and inhibition, ultimately requiring a single Fc-antibody for all protein kinase catalyzed processes. The nonbiological antigen Fc and the highly specific Fc-Ab$_1$ are key to our approach detailed here. Limited reports of Fc-Ab$_1$ have appeared in the

Received: March 16, 2012
Published: July 5, 2012

   dx.doi.org/10.1021/ja302586q | J. Am. Chem. Soc. 2012, 134, 17036−17045

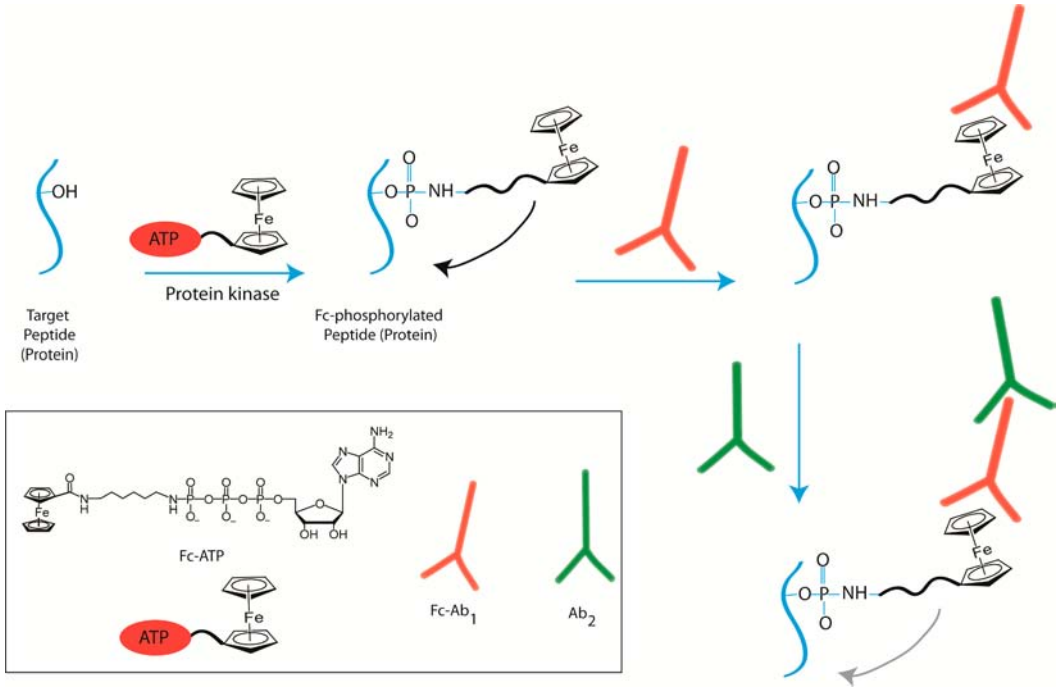

Figure 1. Strategy for Fc-phosphorylation of peptides and proteins. Target peptide or protein is Fc-phosphorylated in the presence of protein kinase and Fc-ATP cosubstrate. This process is successfully measured for the immobilized target by surface electrochemistry. In an immunoassay approach, primary polyclonal anit-ferrocene antibodies (Fc-Ab_1) bind to Fc-phosphates, on surfaces or in solution, specifically followed by fluorescently labeled goat antirabbit antibodies (Ab_2) binding in a two-step immunoreaction. On surfaces, the fluorescence imaging of Fc-phosphorylations, in an immunoarrray method, takes advantage of the proposed strategy. Similarly, the immunoreaction principle was utilized in a biochemical approach for Western blotting.

context of immunoprecipitation and as mimics of a cyclic transition state of a Diels–Alder reaction.[17]

Here we describe how we utilize Fc-Ab_1 as a versatile bioanalytical tool for developing a new biosensing strategy able to monitor phosphorylation reactions of Thr/Ser/Tyr residues in peptides or proteins. In a biochemical assay, we apply the Fc-Ab_1/Ab_2 system for visualization of the protein kinase-driven transfer of the γ-Fc-phosphate group from Fc-ATP to the hydroxyl group of a peptides or proteins, and compare the reaction kinetics of Fc-ATP versus ATP. In addition, we carry out a head-to-head comparison of the Fc-ATP conjugate and its performance in cell lysate with the standard [γ-^{32}P]ATP radiolabel. Comparative inhibition studies for ATP and Fc-ATP were also performed. This report clearly demonstrates the utility of Fc-Ab_1 in combination with Fc-ATP for probing phosphorylation of peptides and proteins in solution and on surfaces, which may find use in the field of proteomics and pharmaco-proteomics.

EXPERIMENTAL SECTION

Methods. All reagents and chemicals were used as received unless otherwise specified. Serum enriched with polyclonal rabbit anti-ferrocene antibodies (Fc-Ab_1) were produced at the YenZym Antibodies, LLC (CA, U.S.) against the monosubstituted ferrocene-amide-alkylamine. Fc-Ab_1 was used without further purification and used at 1:10 000 in 0.1% bovine serum albumin (BSA) in Tris buffer saline Tween20 (TBST), unless otherwise specified. Fluorescently labeled secondary goat antirabbit antibodies GAR 800, GAR 600, GAM 800, and GAM 600 (Ab_2) were purchased from the Biocompare (NJ, U.S.) and were used at 1:10 000 dilution. Au on silicon sputtering wafers were obtained from the Nanofabrication facility at Western University and were used for TOF-SIMS and XPS analyses, as well as for the fluorescence assays. Polycrystalline gold disk electrodes (0.02 cm2) were purchased from CHInstruments and were used for all electrochemical studies. The surface roughness factor and the associated reproducibility were previously estimated to be 1.2 ± 0.2 and 10–20%, respectively.[18] Surface Plasmon resonance (SPR) array chips were purchased from the GWC Technologies (WI, U.S.) and were used without further cleaning. All SPR experiments were performed on a SPRimager (GWC Technologies, USA) using a self-assembled monolayer on a microarray Au-coated glass surface by immersion in the appropriate solutions. A LI-COR Odyssey Imager (LI-COR Biosciences) was used to produce fluorescence images of the microarray slides by monitoring channel 800. Incubation with shaking was achieved with VWR Scientific Model 100 (rocking platform, USA). HeLa cells were cultured as previously described, and the protein content was determined using the BCA method to be 4 mg mL^{-1}. The synthesis of the Fc-ATP was previously reported.[14a]

Synthesis of Fc-BSA. The protocol for the synthesis of Fc-labeled bovine serum albumin (Fc-BSA) was based on the modified literature procedure.[19] To a stirred solution of BSA (0.1 g, 1.5 μmol) in 50 mM potassium phosphate buffer (pH 7.4) (3 mL) was dropwise added a solution of ferrocene *N*-hydroxysuccinimide ester (0.05 g, 0.14 mmol) in anhydrous dimethylformamide (DMF) (0.07 mL). The reaction mixture was stirred at 25 °C overnight and then centrifuged to remove the supernatant. The supernatant was dialyzed for 4 days against 50 mM potassium phosphate buffer (pH 7.4) to remove excess salts and unreacted Fc-compounds. Dialyzed solution contained approximately 500 μM of protein and was used as such for further study. The characterization of Fc-BSA solution was achieved by MALDI-TOF MS and the spectra indicated the formation of the Fc-BSA conjugate with a 4:1 ratio of Fc groups to BSA molecule. Fc-BSA solution of known protein concentration was used as the standard in Western blotting analysis.

Western Blotting. Protein samples were resolved by 10% and 12% SDS–polyacrylamide gel electrophoresis (SDS-PAGE), transferred to polyvinylidene difluoride (PVDF) membranes (Millipore) and subjected to Western blotting analysis. Membranes were blocked in 5% bovine serum albumin (BSA) in TBST for 1 h, followed by

dx.doi.org/10.1021/ja302586q | J. Am. Chem. Soc. 2012, 134, 17036–17045

overnight incubation at 4 °C with the appropriate primary antibody diluted in 1% BSA/TBST. Membranes were washed with TBST and then incubated with the secondary antibodies. After incubation with secondary antibody, the membranes were washed with TBST and visualized with the LI-COR imager.

Serial Dilutions of Fc-BSA. Fc-BSA was serially diluted in water with concentrations ranging from 1 μg to 1 pg and subjected to Western blotting analysis as previously described. Bands were quantified using LI-COR Odyssey Software (LI-COR Biosciences) and graphed using performed using GraphPad Prism version 5.00. Assays were done in triplicates.

Phosphorylation of His-Procaspase 3. His-tagged inactive procaspase 3 C163A (Addgene plasmid 11822, Caspase-3) and GST-tagged CK2α were purified from *Escherichia coli* as described.[19] For the phosphorylation reaction, 1 μg His-procaspase 3 C163A was phosphorylated by 100 ng GST-CK2α in CK2 kinase assay buffer (50 mM Tris-HCl (pH 7.5), 150 mM NaCl, 10 mM $MgCl_2$) using either 100 μM ATP or 100 μM FcATP. The reactions were incubated for 1 h at 30 °C with shaking and stopped by boiling in sample buffer. Phosphorylation was analyzed by Western blotting analysis.

Development of Phospho-Caspase 3 Antibody. Phospho-specific caspase-3 antibodies were generated against GIEpTDpSGVDDMAC by YenZym Antibodies, LLC (San Francisco, CA) using proprietary methods.[20]

Substrate Concentration Studies. To further our kinetic characterization, increasing concentrations of C-terminal 6x His tagged caspase 3 C163A (0−25 μM) were incubated with 100 ng GST-CK2α in CK2 kinase assay buffer with either 100 μM ATP or FcATP for 15 min at 30 °C with shaking and stopped by boiling in sample buffer. To control for nonphospho-specific binding of antibodies due to increasing substrate concentrations, phosphorylation was assayed with and without the addition of either ATP or FcATP. Phosphorylation was detected with phosphor-caspase 3 antibodies or Fc-Ab_1. Phosphorylation was analyzed by Western blotting analysis and quantified by using LICOR Odyssey software. Kinetic parameters were calculated using nonlinear regression with GraphPad Prism version 5.00. Assays were done in triplicate.

General Protein Phosphorylation Reactions. To biochemically test for variety of protein phosphorylations, different protein constructs were tested. A 1-μg portion of purified CK2 substrates α-casein (E.H. Ball, Western University, Canada), C-terminal 6x His tagged caspase 3 C163A, N-terminal 6x His tagged caspase 8 C360A, N-terminal 6x His tagged caspase 8 C360A (Addgene plasmid 11828), and caspase 8 C360A T373A, were incubated with 100 ng GST-CK2α in CK2 kinase assay buffer and either 100 μM ATP supplemented with 10 μCi [γ-^{32}P]ATP (3000 Ci/mmol) or 100 μM FcATP for 30 min at 30 °C with shaking and stopped by boiling in sample buffer. Proteins were resolved by SDS-PAGE. Fc-phosphorylation was detected by Fc-Ab_1 in Western blotting analysis. ATP phosphorylation was detected using a phosphorimager.

Inhibition Studies. The inhibition studies were performed in the presence of 4,5,6,7-tetrabromo-1H-benzotriazole (TBB), 2-dimethylamino-4,5,6,7-tetrabromo-1H-benzimidazole (TBBz), and E-3-(2,3,4,5-tetrabromo-mophenyl)acrylic acid (DMAT). GST-CK2α was incubated on ice for 18 min with increasing concentrations of CK2 inhibitors TBBz, TBB, and DMAT (0.006−60 μM). A 100-ng portion of GST-CK2 plus inhibitor was diluted 5-fold into kinase reactions containing 1 μg C-terminal 6xHis tagged caspase 3 C163A in CK2 kinase assay buffer and either 100 μM ATP or FcATP. Reactions were incubated at 30 °C for 30 min with shaking and stopped by boiling in sample buffer.

Proteins were resolved by SDS-PAGE and phosphorylation was analyzed by phospho-caspase 3 antibodies (Phospho-C3) or Fc-Ab_1 and Western blotting analysis. Phosphorylation was quantified by using LICOR Odyssey software. Relative inhibition was graphed with GraphPad Prism version 5.00. Assays were done in triplicate.

Co-Substrate Concentration Studies. The cosubstrate concentration studies were performed by incubating 1 μg His-procaspase 3 C163A (Caspase-3) with 100 ng GST-CK2α in CK2 kinase assay buffer with increasing concentrations of FcATP or ATP (10 − 500 μM). The reactions were incubated for 15 min at 30 °C with shaking and stopped by boiling in sample buffer. Phosphorylation was analyzed by Western blotting analysis. Phosphorylation was quantified using LI-COR Odyssey software. Kinetics parameters were calculated using nonlinear regression with GraphPad Prism version 5.00. Assays were done in triplicate.

Lysate Phosphorylation. In vitro studies were performed by incubating 10 μg HeLa lysate with either 1 mM ATP supplemented with 10 μC [γ-^{32}P]ATP (3000 Ci/mmol) or 1 mM FcATP in CK2 kinase assay buffer for 1 h at 30 °C with shaking, and the reaction stopped by boiling in sample buffer. As a control, 200 mM EDTA was added to the reaction to inhibit kinase-catalyzed phosphorylation. Proteins were resolved by SDS-PAGE and transferred to PVDF membranes. Fc-phosphorylation was analyzed by Western blotting analysis with Fc-Ab_1, whereas ATP phosphorylation was detected with a phosphorimager (Molecular Dynamics). Relative phosphorylation was determined with ImageQuant TL software (Amersham Biosciences). Assays were done in triplicate.

Substrate Cleaning and Preparation. All electrochemical experiments were performed using Au disk electrodes. The surface characterization and fluorescence experiments were performed using Au on silicon sputtering wafers (~0.5 × 4 cm or 2 × 2 cm for array studies). Au wafers were marked by etching alongside the top and the right side of the plate to allow for proper positioning of the spots. The cleaning of the Au wafers was achieved by etching in *pirhana* solution (3:1%vv H_2SO_4: H_2O_2, 3 min), rinsing with Milli-Q water, sonicating in freshly distilled ethanol (10 min), and drying under N_2.

Peptide and Protein Film Formation on Au Substrates. The Au substrates were immersed in 2 mM lipoic-NHS acid ester (Lip-NHS) for 2 days at 5 °C. After rinsing with ethanol, the Au substrates were spotted with 5 μL of the target protein or peptide sequence (100 μM aqueous solution unless otherwise specified) to form 8−16 spots and incubated at 5 °C overnight.

Ferrocenyl Phosphorylation of Surface-Bound Targets on Au Substrates. The kinase catalyzed Fc-phosphorylation reactions were performed in the kinase assay buffer. The buffer composition used was similar to that suggested by the kinase provider with omission of DTT. Following target peptides were used: Glu-Gly-Ile-Tyr-Asp-Val-Pro, His-His-Ala-Ser-Pro-Arg-Lys, Arg-Arg-Leu-Ser-Ser-Leu-Arg-Ala, Arg-Arg-Arg-Asp-Asp-Asp-Ser-Asp-Asp-Asp, and Glu-Pro-Leu-Thr-Pro-Ser-Gly. The protein investigated were α-casein and caspase-3.

Sarcoma (Src) kinase, Cyclin-dependent kinase (CDK2), casein kinase II (CK2), Erk1 and protein kinase A (PKA) were used in the phosphorylation reactions. Typically, a phosphorylation reaction was performed using the protein kinase (1 μg mL^{-1}) and Fc-ATP (200 μM) in the kinase assay buffer, unless otherwise mentioned. The kinase reaction was spotted (0.4 μL) on the predetermined peptide spots on the Au plate. All kinase assays were performed at 37 °C for 2 h to ensure the maximum Fc-phosphate coverage. The microarray plates were rinsed with kinase buffer prior to immunoreactions. Other concentration studies were performed in a similar manner in the presence of increasing PKA kinase concentration: 0, 0.1, 0.5, and 1 μg mL^{-1}, increasing CK2 concentration: 0, 0.1, 0.2, 0.3, 0.5, and 1 ng mL^{-1} or increasing Fc-ATP concentration: 0, 5, 10, 20, 50, 100, and 200 μM.

Inhibition studies were also performed in a fluorescence array format at 5 μM TBB, TBBz, and DMAT.

The control studies were performed in the presence of ATP (200 μM).

Surface kinetics associated with the kinase-catalyzed phosphorylation was evaluated using the Michael-Menten equation with respect to the cosubstrate Fc-ATP, and surface enzyme-catalyzed reactions with respect to the CK2 protein kinase.

Electrochemical Experiments. In a typical electrochemical experimental set-up a Fc-film or peptide-modified Au electrode was used as a working electrode, Ag/AgCl in 3 M KCl as the reference electrode, and a platinum wire as the counter electrode. All cyclic voltammetry (CV) and square-wave voltammetry (SWV) experiments were carried out using a CHInstrument potentiostat 660B (Austin,

TX), 0.2−0.6 V potential range, and 0.1 sodium phosphate buffer, pH 7.4. All electrochemical measurements were performed in duplicate.

Immunoarray Fluorescence Imaging. Following the surface-assisted phosphorylation on Au surfaces, the substrates were immersed in the LI-COR blocking reagent for 1 h at RT to further eliminate the nonspecific binding of the antibodies. The substrates were rinsed in TBST (5 min) and incubated in a primary Fc-Ab solution (1:100 or 1:1000 dilution in 0.1%BSA/TBST) for 1 h at RT. The Au substrates were then rinsed twice with TBST (5 min) and subsequently incubated with secondary goat antirabbit antibody (Ab_2, GAR 800, 1:10 000 dilution in 0.1%BSA/TBST) for 45 min at RT. The substrates were then rinsed twice with TBST and twice with TBS and imaged using the LI-COR imager.

Surface-Plasmon Resonance Experiments. The 25-SPR array chip was immersed in 2 mM lipoic-NHS acid ester for 2 days at 5 °C. After rinsing with ethanol, the array was spotted with 0.3 μL of the target peptide sequence Arg-Arg-Arg-Asp-Asp-Asp-**Ser**-Asp-Asp-Asp (100 μM in ddH_2O) and incubated in a humid chamber at 5 °C for 16 h. The plates were then rinsed with ddH_2O and dried under nitrogen. The peptide arrays were treated with the kinase reaction mixture containing CK2 protein kinase: 0, 0.1, 0.2, 0.3, 0.5, and 1.0 ng mL^{-1} and Fc-ATP (200 μM) for 2 h at 37 °C. The control studies were performed in the presence of ATP (200 μM) and CK2 (1.0 ng mL^{-1}). The SPR arrays were subsequently washed and treated with the LI-COR blocking solution for 1 h at 25 °C and further washed with TBST. The peptide arrays were placed into an SPR instrument and the buffer (0.1% BSA/TBST) was applied to the array surface at 200 μL min^{-1} for 6 min. The array was then treated with Fc-Ab_1 solution (1:1000 dilution in 0.1%BSA/TBST) for 8 min and followed with the buffer for 6 min. The binding was given in the response units (RU) as a function of time for each ROI. The plots were generated from the normalized RU values estimated after the addition of Fc-Ab_1 and signal stabilization. SPR data was fitted to the surface-based kinetic model to estimate K_M.[20] The association and dissociation rate constants were estimated from SPR data by assuming the single binding model and a fitting software kindly provided by the GWC Technologies.

Time-of-Flight Secondary Ion Mass spectrometry (TOF-SIMS). Samples for TOF-SIMS analysis were prepared as previously described. Au substrates were cleaned and immersed in the Lip-NHS solution, followed by immobilization of a peptide (Arg-Arg-Arg-Asp-Asp-Asp-Ser-Asp-Asp-Asp) or a protein (caspase-3). Each substrate was subsequently Fc-phosphorylated in the presence of CK2 and Fc-ATP. Subsequently, the Fc-phosphorylated films were exposed to Fc-Ab_1. TOF-SIMS experiments were performed with TOF-SIMS IV (ION-TOF GmbH, Munster, Germany). For all measurements, a 25 keV $Bi3^+$ cluster primary ion beam with a pulse width of 12 ns was employed (target current of ~1 pA). The cycle time for the processes of bombardment and detection was 100 μs (or 10 kHz) was used. A pulsed, low energy electron flood was used to neutralize the sample charging. For each sample, spectra were collected from 128 × 128 pixels over an area of 500 × 500 μm for 60 s. The positive and negative secondary ions were extracted from the sample surface, mass separated, and detected via a reflectron-type of time-of-flight analyzer, allowing parallel detection of ion fragments having a mass/charge ratio up to 900 within each cycle (100 μs). Positive and negative ion spectra were internally calibrated by using H^+, H_2^+, and CH_3^+ and H^-, C^- and CH^- signals, respectively. Two spots per sample were analyzed using a random approach.

X-ray Photoelectron Spectroscopy. Au substrates were cleaned and immersed in the Lip-NHS solution followed by immobilization of a peptide (Arg-Arg-Arg-Asp-Asp-Asp-Ser-Asp-Asp-Asp) or a protein (caspase-3). Each substrate was subsequently Fc-phosphorylated in the presence of CK2 and Fc-ATP. Subsequently, the Fc-phosphorylated films were exposed to Fc-Ab_1. The samples were analyzed by Kratos Axis Ultra X-ray photoelectron spectrometer using a monochromatic Al Kα source (15 mA, 14 kV). The instrument was calibrated to give the binding energy (BE) of 83.96 eV for the Au 4f7/2 line for metallic gold and the spectrometer dispersion was adjusted to give BE of 932.62 eV for the Cu 2p3/2 line of metallic copper. The Kratos charge neutralizer system was used on all samples. Survey scan analyses were carried out with an analysis area of 300 × 700 μm and a pass energy of 160 eV. High-resolution analyses were carried out with an analysis area of 300 × 700 μm and a pass energy of 20 eV. Spectra have been charge corrected to the main line of the C1s spectrum (adventitious carbon) set to 284.8 eV. Spectra were analyzed using CasaXPS software (version 2.3.14).

RESULTS AND DISCUSSION

Ferrocenyl-Phosphorylations in Solutions: Biochemical Approach. First, the Fc-Ab_1 was characterized with respect to the dynamic range and working concentrations in a standard biochemical assay (Figure 2a). For this study, Fc-BSA

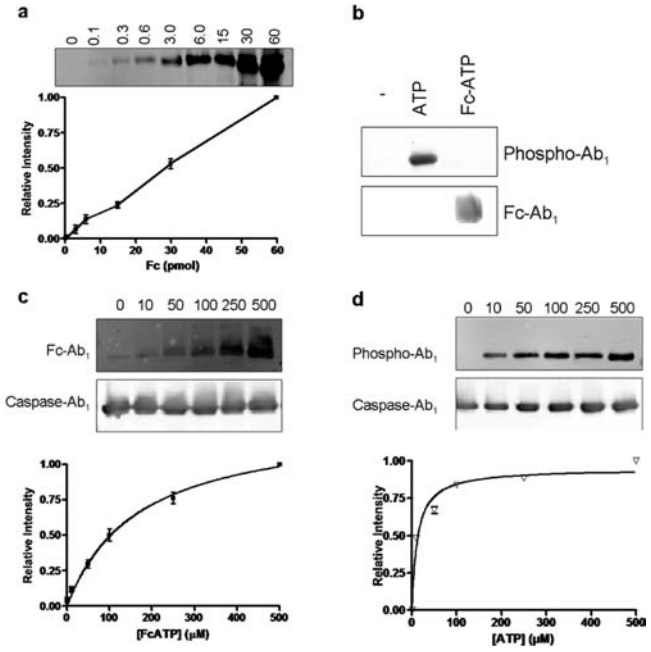

Figure 2. Fc-Ab_1 characterization and the phosphorylation of caspase-3. (a) Characterization of Fc-Ab_1 by varying the concentration of Fc-BSA (0−60 pmol). (b) Phosphorylation of caspase-3 by ATP and Fc-ATP and detection by Phospho-caspase Ab_1 and Fc-Ab_1. (c) Fc-phosphorylation as a function of Fc-ATP (0−500 μM). (d) Phosphorylation as a function of ATP (0−500 μM).

was synthesized according to the literature protocol[19] and used at varying concentrations (0−60 pmol) and the signal was measured following the incubation with Fc-Ab_1 and Ab_2.

The limit of detection was estimated to be 30 fmol Fc-BSA, which translates into 120 fmol of Fc as there are 4 Fc per BSA molecule. This represents the appropriate working range to study phosphorylation reactions which was explored next. The phosphorylation and Fc-phosphorylation of His-tagged inactive procaspase 3 C163A (caspase-3) by casein kinase II (CK2) were detected by phospho-Ab_1 and Fc-Ab_1 as shown in Figure 2b. CK2 has been implicated in cancer since it is often overexpressed, and one of its targets is caspase.[20,21] Other proteins, such as α-casein and caspase-8 were successfully Fc-phosphorylated by Fc-ATP indicating the utility of Fc-ATP and the generality of the Fc-Ab_1 assay (Supporting Information, Figures S8−9). Additionally, when Thr 373 of caspase-8 is mutated to an Ala no phosphorylation was detected with both ATP and Fc-ATP. The pattern of phosphorylation between these substrates is comparable for ATP and Fc-ATP and follows the phosphorylation order: α-casein > caspase-3 > caspase-8.

dx.doi.org/10.1021/ja302586q | J. Am. Chem. Soc. 2012, 134, 17036−17045

Notably, no cross reactivity was observed for Fc-Ab_1 with phosphorylated and unphosphorylated protein samples.

Importantly yet, phospho-Ab_1 does not bind Fc-phosphorylated protein which provides an opportunity to utilize two different antibodies for complex analysis. There was no background signal observed when either ATP or Fc-ATP was omitted from the reaction.

The phosphorylation reactions were further explored with respect to ATP and Fc-ATP concentrations. In Figure 2c, the saturation in Fc-phosphorylation was observed at 500 μM Fc-ATP. From the reciprocal plots of reaction velocity versus Fc-ATP concentrations, the K_M value was determined to be 165 $\pm$ 24 μM. Similarly, K_M value was determined for ATP reaction (Figure 2d) and estimated to be 12 $\pm$ 2 μM, which is consistent with values previously reported in the literature.[22]

The caspase-3 concentration dependent experiments were carried out and indicate the increase in the phosphorylation levels by ATP (Figure 3a) or Fc-ATP (Figure 3b) as the substrate concentration is increased. From the nonlinear regression plots, the K_M values, with respect to caspase-3 substrate, were determined to be ~1.32 $\pm$ 0.15 and 1.40 $\pm$ 0.19 μM for ATP and Fc-ATP, respectively, and are statistically similar.

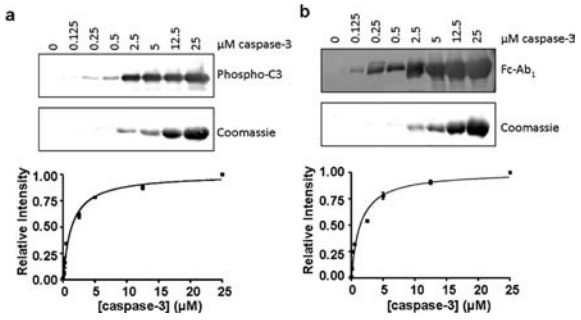

Figure 3. Comparative cosubstrate phosphorylation studies. Phosphorylation reactions in the presence of GST-CK2α and (a) ATP and (b) Fc-ATP as a cosubstrate at caspase-3 concentrations of 0, 0.125, 0.25, 0.5, 2.5, 5, 12.5, and 25 μM. Total protein content was detected with the Coomassie blue stain, the phosphorylated protein was detected with the phospho-caspase 3 antibodies (Phospho-C3) and Fc-phosphorylated protein was detected with Fc-Ab_1.

Comparing this data to the kinetics with increasing ATP or Fc-ATP cosubstrate concentrations, it is evident that CK2 has a lower affinity for Fc-ATP than ATP (different K_M values with respect to the cosubstrate) but has a similar ability to phosphorylate capase-3 substrate (similar K_M values with respect to the substrate). Next, the utility of Fc-ATP was explored with respect to whole cell lysate phosphorylations and compared to ATP reactions. In the presence of phosphatase and protease inhibitors and excess cosubstrate concentration, the phosphorylation reactions were performed for 1 h at 30 °C. The phosphorylation patterns in Figure 4a,b suggest that Fc-ATP is widely used by protein kinases inherent to the cell lysate to phosphorylate a number of proteins. Notably, the phosphorylation and Fc-phosphorylation trends are similar, but a slight difference exists in the lower molecular weight range. Additionally, these bands are specific to Fc-phosphorylated cellular proteins as no background bands are present in the cell lysate and antibody control lanes. Furthermore, these bands are specific to kinase-catalyzed Fc-phosphorylation as

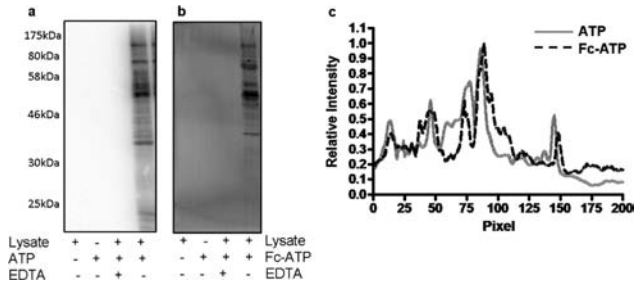

Figure 4. Phosphorylation of whole cell lysates. (a) Autoradiograph of phosphorylation reactions of cell lysates. (b) Western blot of Fc-phosphorylation reactions of cell lysates. (c) Plots of relative intensity, taken from the blots, versus pixel for phosphorylation reactions with Fc-ATP and ATP.

incubation in the presence of EDTA prevents phosphorylation, demonstrated by the absence of bands (Figure 4a,b).

Since the protein kinases are drugable biological targets, screening for the kinase inhibitors is of interest and was probed next with Fc-Ab_1. For inhibition of CK2 kinase, 4,5,6,7-tetrabromo-2-azabenzimidazole (TBB), 2-dimethylamino-4,5,6,7-tetrabromo-1*H*-benzimidazole (TBBz), and *E*-3-(2,3,4,5-tetrabromo-mophenyl)acrylic acid (DMAT) inhibitors were chosen due to their well-known inhibitory activity.[23] The CK2 inhibition studies were also performed with ATP and Fc-ATP and caspase-3 as a cosubstrate (Figure 5).

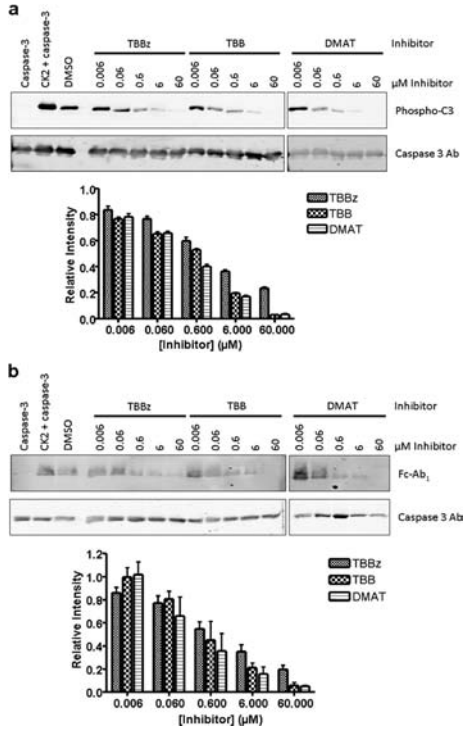

Figure 5. Comparative cosubstrate inhibition studies. (a) ATP and (b) Fc-ATP cosubstrates used in the phosphorylation reactions of caspase-3 in the presence of GST-CK2α and inhibitors TBB, TBBz, and DMAT. Inhibitor concentrations: 0, 0.006, 0.06, 0.6, 6, and 60 μM. Total protein content was detected with the caspase-3 antibodies (Caspase 3 Ab), phosphorylated protein was detected with phospho-caspase 3 antibodies (Phospho-C3) and Fc-phosphorylated proteins were detected with Fc-Ab_1.

dx.doi.org/10.1021/ja302586q | J. Am. Chem. Soc. 2012, 134, 17036−17045

In the absence of CK2, no phosphorylation was observed. In the presence of CK2 and the control, dimethylsulfoxide (DMSO) which served as the inhibitor solvent, very small effects on phosphorylation levels were observed for both ATP and Fc-ATP. By adding the increasing amounts of CK2 inhibitors: TBBz, TBB, and DMAT, the phosphorylation levels with ATP and Fc-ATP decreased accordingly. The relative phosphorylation intensities were compared to the inhibitor-free runs and plotted. In the case of ATP and Fc-ATP, TBB, and DMAT appeared to be better inhibitors than TBBz. Overall, the inhibition profiles for all three inhibitors are similar for ATP and Fc-ATP.

Ferrocenyl-Phosphorylations on Surfaces: Electrochemical and Fluorescence Approach. To explore the utility of Fc-Ab_1 in a biosensing format, we next targeted an enzymatic reaction on the surface, which utilizes the Fc-ATP as a cosubstrate. Toward this goal, the clean Au surface was incubated in a solution of 2 mM lipoic *N*-hydroxysuccinimide ester (Lip-NHS) and conjugated to a short target peptide or protein.[24] The peptide- and protein-modified Au surfaces were exposed to the kinase reaction mixtures containing the Fc-ATP (200 μM) and a CK2 protein kinase (1 ng mL^{-1}). Figure 6a depicts a typical redox signal observed for the Fc-phosphopeptide-modified Au surface and is characterized by a formal potential E^0 at 360 ± 10 mV (versus Ag/AgCl reference electrode). Similar redox activity for other Fc-phosphorylated peptides and Fc-phosphorylated proteins on the Au surfaces were reported earlier.[24] The Fc-phosphorylation of peptides containing Thr/Ser/Try residues, by a variety of protein kinases, has been demonstrated using the Fc-ATP cosubstrate using electrochemical measurements. For example, we demonstrated Fc-phosphorylation of the immobilized peptide sequences by a variety of protein kinases including sarcoma-related kinase (Src), protein kinase A (PKA), protein kinase C (PKC), Abl kinase, Her2 kinase, cyclin-dependent 2 kinase (CDK2), Erk1 kinase, glycogen-synthase kinase, and CK2 kinase, indicating that Thr/Ser/Tyr residues may be modified using Fc-ATP cosubstrate and monitored by electrochemical means.[24,25] In general, the electrochemical determination of the Fc-ATP cosubstrate kinetics resulted in the K_M values in the 20−200 μM range, depending on the protein kinase used, which are overall lower than the corresponding ATP values.[24,25] Hence, the protein kinases have lower affinity for Fc-ATP than ATP. The biochemical assays further support this trend as shown above. Notably, sub-mM concentrations of Fc-ATP may not be well tolerated by other protein kinases. The electrochemical signal-on response, previously observed for the Fc-phosphorylated peptide films, may be attenuated in the presence of the specific Fc-Ab_1, which offers a secondary confirmation of the successful Fc-modifications. Incubation with Fc-Ab_1 at 1:1000 dilution resulted in a 6-fold current reduction due to the binding of Fc-Ab_1 to the Fc-groups on the surface. The fluorescence imaging was achieved by Ab_2 to visualize the two distinctly different surfaces. The fluorescence images of the unphosphorylated and phosphorylated peptide films are shown in Figure 6b (top). In the control experiment, in the absence of Fc-phosphoryalation, Fc-Ab_1 does not bind the peptide spot on the surface. Clearly, the nonphosphorylated films are only weakly fluorescent following the treatment with Fc-Ab_1 and labeled Ab_2. Moreover, there was no nonspecific binding to a bare Au surface, ethanolamine layer and hexanethiol background. By contrast, the Fc-phosphorylated film is characterized by the relatively strong fluorescence judging by the average fluorescence intensities (Figure 6b (bottom)). For the background-subtraction, the Au surface with Lip-NHS, ethanolamine and hexanethiol layers was used as the reference.

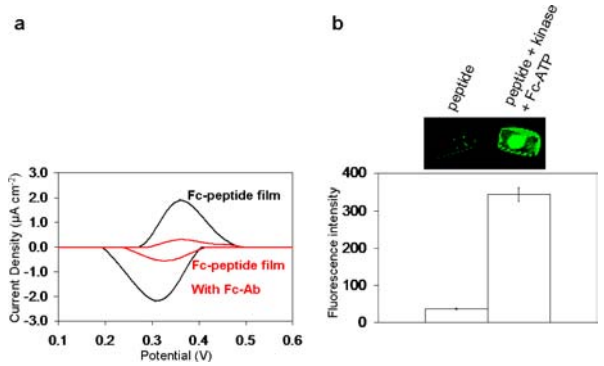

Figure 6. Immuno-electrochemical detection of Fc-phosphorylation of immobilized peptides. (a) Background-subtracted cyclic voltammograms of the Au surfaces containing the Fc-phosphorylated peptide film before and after addition of Fc-Ab_1 (1:1 000). (b) Fluorescence images (top) of peptide-modified and Fc-phosphopeptide-modified Au surfaces following the addition of Fc-Ab_1 (1:1 000) and fluorescent Ab_2 (1:10 000). Plot of the average fluorescence intensities versus film type (bottom b) taken from the images (intensities were estimated from the average fluorescence intensities and errors were estimated from duplicate measurements).

The fluorescence signal is related to Ab_2 that targets Fc-Ab_1 which binds the Fc-groups on the surface. For the peptide-modified Au, the intensity ratio for the unphosphorylated to Fc-phosphorylated films was close to a factor of 10. These proof-of-concept studies demonstrate the utility of Fc-Ab_1 for monitoring Fc-phosphorylations on two separate Au surfaces, however, monitoring multiple kinase reactions on a single chip is desirable.

We have investigated the process of the substrate immobilization, Fc-phosphorylations and antibodies binding on Au surfaces by a variety of surface-based characterization techniques, such as time-of-flight secondary ion mass spectrometry (TOF-SIMS) and X-ray photoelectron spectroscopy (XPS). From the TOF-SIMS spectra, the ion intensities of interest were compared for different samples ranging from (a) bare Au surface to Au surfaces with the following modifications: (b) Lip-NHS, (c) conjugated peptide, (d) conjugated protein, (e) Fc-phosphorylated peptide, (f) Fc-phosphorylated protein, (g) Fc-Ab_1 bound to Fc-phosphorylated peptide, and (h) Fc-Ab_1 bound to Fc-phosphorylated protein. The overall intensities for Fe^+ ions in the positive TOF-SIMS spectra (Figure 7a) clearly show the presence of the iron content following the Fc-phosphorylations of the immobilized peptide or protein (e,f). No iron was detected in the non-Fc-phosphorylated samples (a−d). Notably, the subsequent binding of the Fc-Ab_1 to the Fc-films, results in a dramatic decrease in the Fe^+ ion intensities. Antibody/Fc interactions will increase the film thickness, resulting in lower ion intensities due to limits in penetration depth associated with the measurement.[26] In addition, intensity of Au^- ions decreased (Figure 7a). The bare Au surface (a) is characterized by a high Au- content which decreases upon further surface modifications. After Fc-Ab_1 binding (g,h) to the Fc-films, the Au- ions are dramatically suppressed. Figure 7b shows the relative trends of normalized ion intensities of interest Fe^+, Au^-, and CNO^- as

dx.doi.org/10.1021/ja302586q | J. Am. Chem. Soc. 2012, 134, 17036−17045

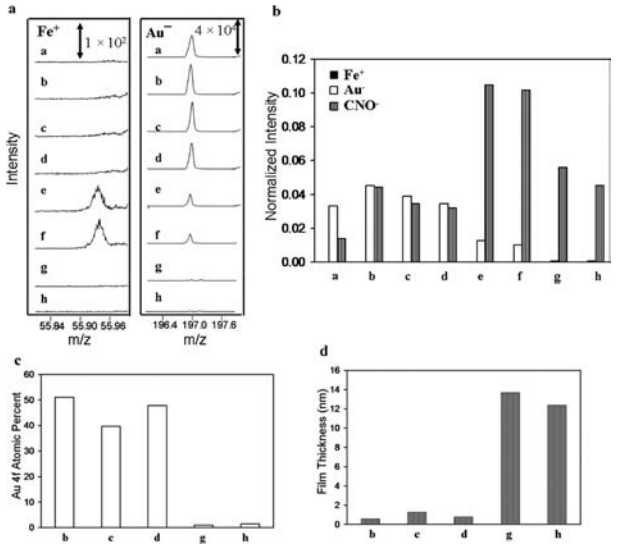

Figure 7. Surface characterization of films on Au surfaces. (a) TOF-SIMS spectra showing Fe^+ and Au- ions. (b) Normalized TOF-SIMS ion intensities: Fe^+, Au^-, and CNO- as a function of the film types. The intensities were normalized to the total ion intensities of the samples. (c) XPS analysis of the Au 4f atomic percent values as a function of film type. (d) Film thickness estimated from the Au 4f area as a function of film type. Film compositions: (a) bare Au surface, (b) Lip-NHS, (c) conjugated peptide, (d) conjugated protein, (e) Fc-phosphorylated peptide, (f) Fc-phosphorylated protein, (g) Fc-Ab_1 bound to Fc-phosphorylated peptide, and (h) Fc-Ab_1 bound to Fc-phosphorylated protein.

a function of film type on Au surfaces. Of particular importance is the intensity of the CNO^- ion, which is related to the organic content of the films. The CNO^- ion content significantly increases with film thickness. Notably, the CNO^-/Au^- ion intensity ratio is greater for the films containing the bound Fc-Ab_1 (76 for (g), and 66 for (h)) than for the antibodies' free films (8 for (e), and 10 for (f)). In addition, all of the films, except bare Au, possess strong S^- ion content, which points to the successful attachment and stability of the Lip-NHS ester and the subsequent surface modifications.

XPS analysis for the different films revealed that sequential surface modifications reduced the intensities associated with the Au 4f core levels. A decrease in the atomic percent of Au 4f is most evident for the Fc-phosphorylated films, which have been incubated with Fc-Ab_1 (Figure 7c). These findings are in strong agreement with the TOF-SIMS analysis. Assuming the average polymer electron attenuation length (EAL),[27] the film thickness was calculated for different films from the XPS intensities of Au 4f and are presented in Figure 7d. The Au percentages, seen from the underlying Au films, suggest that the thickness increases from 1.3 nm for a peptide film to 13 nm upon binding of Fc-Ab_1. Notably, the variations in the film thickness across the surface may influence the XPS estimation. Importantly, the surface characterization and film thickness determination suggest single layer film formation and do not support peptide multilayers.

Ferrocenyl-Phosphorylations in a Fluorescence Immunoarray Format. Next, we focused on preparing peptide immunoarrays on a single Au chip to evaluate the utility of Fc-Ab_1 for screening multiple kinase reactions, protein kinases and their inhibitors. A peptide-array, depicted in Figure 8, was fabricated by manual micropipet-spotting of the target peptides on a Lip-NHS layer on Au substrate (a). All reactions were

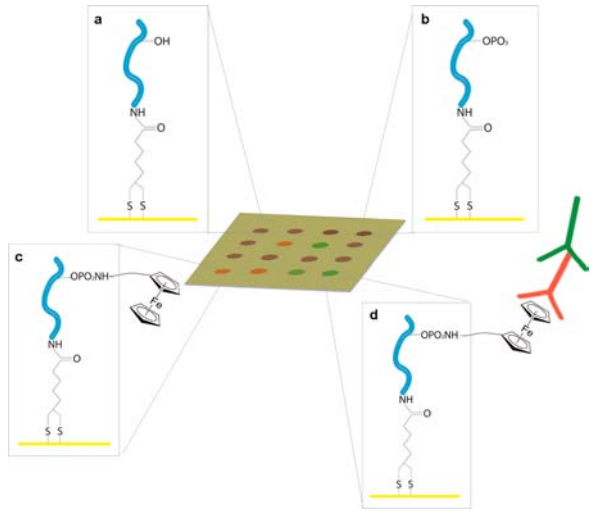

Figure 8. Immunoarray platform for detection of the surface-immobilized phosphorylated peptides. Representation of the peptide array on Au surfaces showing: (a) the discrete peptide spot, and peptide spot following the kinase-catalyzed reaction in the presence of ATP (b) or Fc-ATP (c). Subsequent incubation of peptide array with Fc-Ab_1 followed by addition of fluorescently labeled Ab_2 (d) was used for fluorescence imaging.

performed as described above in the presence of Fc-ATP and the desired protein kinase. The kinase reaction mixture was applied to a given peptide spot on a peptide array.

Following the Fc-phosphorylation reaction, the peptide-arrays were subsequently exposed to Fc-Ab_1 followed by Ab_2 and imaged. Fc-phosphorylation resulted in the transfer of a γ-Fc-phosphate group from Fc-ATP to the immobilized peptide (Figure 8c).

Notably, the reaction spots wherein the kinase-catalyzed phosphorylation was performed in the presence of Fc-ATP will bind the Fc-Ab_1 and Ab_2 as depicted in Figure 8d.

In contrast, the phosphorylation reactions performed in the presence of unmodified ATP will transfer the γ-phosphate group from ATP to the immobilized peptide but will not bind Fc-Ab_1 and Ab_2, as proposed in Figure 8b. Hence, the fluorescence will result only if the appropriate cosubstrate is used.

First, we probed the effects of cosubstrate concentration on the kinase reaction by increasing the Fc-ATP concentrations in the reaction buffer from 0 to 200 μM. Figure 9a shows the image of the peptide-array (Arg-Arg-Arg-Asp-Asp-Asp-**Ser**-Asp-Asp-Asp) following the CK2-catalyzed kinase phosphorylation and the two-step immunoreaction. The fluorescence image in Figure 9a indicates that Fc-Ab_1 binds the Fc-phosphorylated peptide spots rather than the surrounding organic layers. The average fluorescence intensities, extracted from these images were plotted and indicate a saturation level at ~200 μM for Fc-ATP. This finding is comparable to the optimal Fc-ATP concentrations reported using the surface-based electrochemical method.[24] Moreover, a surface-based enzyme model[28] was applied to estimate the Michaelis–Menten constant, K_M, with respect to Fc-ATP to be ~40 μM. Next, the Fc-phosphorylation reaction was evaluated with respect to CK2 protein kinase concentration. From the fluorescence image in Figure 9b the average fluorescence intensities were plotted as a function of CK2 and indicate that 0.2 ng mL^{-1} is the optimal CK2 concentration. Assuming the surface-based

dx.doi.org/10.1021/ja302586q | J. Am. Chem. Soc. 2012, 134, 17036–17045

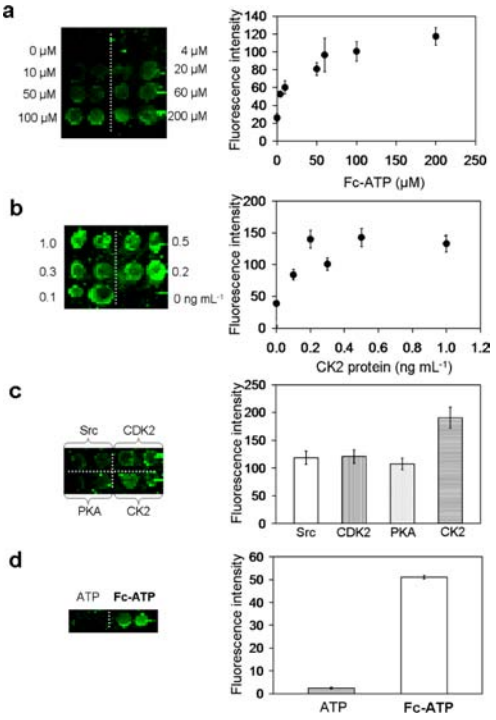

Figure 9. Evaluation of Fc-Ab_1 in an immunoarray format. Fluorescence images (left) and the fluorescence intensities (right) of a single Au array treated with the target peptides and following the kinase-catalyzed phosphorylation reactions in the presence of (a) variable Fc-ATP concentrations, (b) variable CK2 concentrations, (c) variable protein kinases and (d) ATP as a cosubstrate. Au surfaces were exposed to Fc-Ab_1 and labeled secondary Ab_2. Intensities were estimated from normalized data of average intensities and error bars represent duplicate measurements. Dotted lines in images are used to visually separate the series of two spots on the left and right-hand side on the same chip.

enzyme kinetics, the surface Michaelis–Menten constant, K_M, for the protein kinase was determined to be 0.1 ng mL^{-1}.

To address the generality of the Fc-Ab_1 platform, a variety of the peptide substrates and protein kinases were investigated on a single peptide array. For example, the peptide array containing the following short peptides Glu-Gly-Leu-**Tyr**-Asp-Val-Pro, His-His-Ala-**Ser**-Pro-Arg-Lys, Arg-Arg-Leu-**Ser**-**Ser**-Leu-Arg-Ala, and Arg-Arg-Arg-Asp-Asp-Asp-**Ser**-Asp-Asp-Asp were used for kinase-catalyzed phosphorylation reactions by Src kinase, CDK2, CK2, and PKA, respectively. These protein kinases are commonly overexpressed kinases in cancer cells or cell cycle regulators and drive the phosphorylation of different amino acid residues (Ser and Tyr).[29] Figure 9c depicts an image of the peptide array (left) following the Fc-phosphorylation reactions in the presence of four different kinases. The average fluorescence intensities (right) vary with the protein kinase used and follow the order observed by using the surface-peptide electrochemical approach.

Using Fc-Ab_1, multiple phosphorylation sites can be detected by a single antibody which cannot be achieved using more conventional antiphospho immunoassays, which require specific antibodies for each of the phosphorylated targets.

The cross-reactivity of Fc-Ab_1 with phosphorylations performed in the presence of unmodified ATP was also addressed. No fluorescence was observed after the treatment with Fc-Ab_1 and Ab_2 (Figure 9d). Our data suggest that the Fc-Ab_1 is highly specific to Fc-phosphorylated films and it does not bind the phosphorylated peptides.

Next, Fc-Ab_1 methodology was applied to a SPR 25-array chip to compare the ability of the Fc-Ab_1 to function as a probe in the standardized kinase assay. SPR is a label-free method often used to study protein interactions.[30] Initial protein kinase SPR studies reported on the use of the immobilized antibodies to capture protein kinases and study their interactions with potential inhibitors on the surface.[30a] Alternatively, antiphospho antibodies were used for binding to the phosphorylated peptides and proteins and monitored by SPR.[31]

The need for multiple antibodies in a phosphopeptide SPR array was recently bypassed by a more universal detection approach based on a small biotin-labeled phosphoreceptor and streptavidin.[30,31] In the present system, we use an SPR array format for the first time in two distinct ways in order to monitor protein kinase-catalyzed phosphorylation reactions. Target peptides were immobilized on the SPR as described above. The Fc-phosphorylation reactions were performed as per usual on an SPR peptide-array substrate in the presence of increasing CK2 concentrations (0–1 ng mL^{-1}) and Fc-ATP (200 μM).

In the first approach, a conventional SPR response was monitored to gauge utility of Fc-Ab_1. The arrays were evaluated by SPR imaging with injection of the buffer until a stable response signal (RU) was obtained. To analyze the level of the peptide phosphorylation by SPR, the addition of Fc-Ab_1 was monitored followed by rinsing with buffer until a stable signal was achieved. The association, k_{on}, and dissociation, k_{off}, rate constants were estimated to be 0.0143 M^{-1} s^{-1} and 0.009 s^{-1}, respectively, by assuming a reversible Langmuir 1:1 binding model. The kinetics of Fc-Ab_1 binding are relatively slower than those of the protein–protein reactions such as the association of SH2 domains with the phosphotyrosine peptide ligand (k_{on} = 10 000 M^{-1} s^{-1}).[31] With the rate constants estimated, the corresponding dissociation equilibrium constant K_D was determined to be 820 nM. Following the injection sequence, the SPR response unit (RU) was normalized and plotted as a function of the CK2 protein kinase concentration used in the kinase assay as depicted in Figure 10a.

Assuming the surface-based enzyme kinetics, the surface Michaelis–Menten constant K_M value was determined to be 0.7 ng mL^{-1} by fitting the RU data to the appropriate model. In addition, there was a good correlation (R^2 = 0.9543) between CK2 concentration (0–0.5 ng mL^{-1}) and the level of Fc-Ab_1 binding. Similar linearity (R^2 = 0.9750) was observed between the SPR signal and the Fc-ATP concentration (0–200 μM). The linear dependence of the SPR response due to Fc-Ab_1 binding as a function of the cosubstrate and protein kinase concentration suggests that the Fc-Ab_1 binding is sufficient to monitor the phosphorylation by conventional methods, such as SPR. The methodology may be applied to Ser, Thr, and Tyr phosphorylations of peptides and proteins.

In the second approach, the SPR arrays treated with Fc-Ab_1, as mentioned earlier, were exposed to the fluorescent Ab_2 for imaging. The image of the SPR array is presented in Figure 10b and shows the peptide spots in the absence and presence of the protein kinase. Importantly, the kinase reactions performed in the presence of unlabeled ATP show minimal fluorescence intensities. From the average fluorescence intensities versus CK2 concentration shown in Figure 10c and assuming the surface-based model, K_M value for CK2 protein kinase was estimated to be 0.2 ng mL^{-1}. The K_M values estimated from

dx.doi.org/10.1021/ja302586q | J. Am. Chem. Soc. 2012, 134, 17036–17045

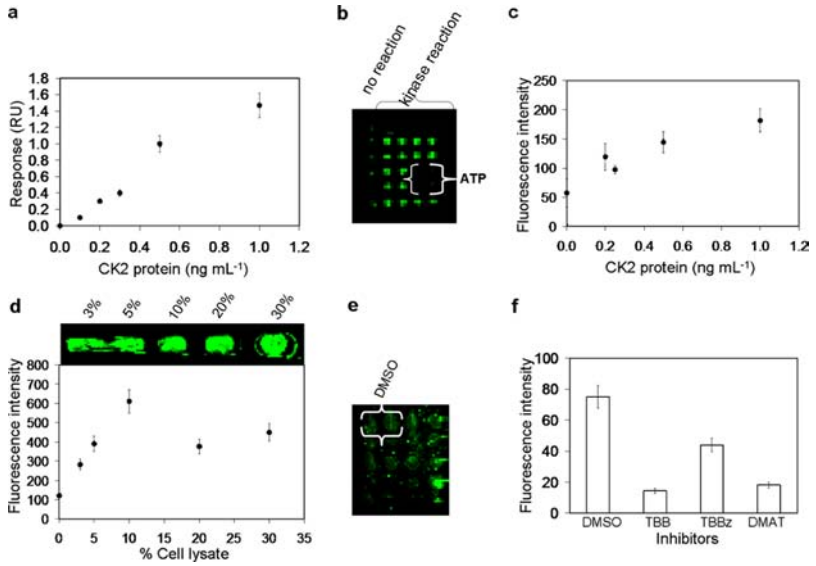

Figure 10. Application of the Fc-Ab_1 for SPR, cell lysates, and inhibitor screening studies. (a) Plot of RU for the peptide films treated with variable CK2 protein kinase concentrations and in the presence of Fc-ATP (200 μM). RU is the normalized response observed after the addition of Fc-Ab_1. (b) Fluorescence image of the SPR array containing the peptide films before and after the kinase reactions with CK2 at variable concentrations in the presence of Fc-ATP or ATP. SPR array was treated with Fc-Ab_1 followed by fluorescent Ab_2. (c) Plot of fluorescence intensity as a function of CK2 concentrations. Intensities were estimated from the average fluorescence intensities and error bars represent the percent error of duplicate measurements. (d) Fluorescence image (top) of a single peptide-modified Au substrate following the CK2 kinase-catalyzed phosphorylation reactions in the presence of increasing cell lysate content (%vv). Fluorescence intensities versus phosphorylation reaction type (bottom). All surfaces were exposed to the Fc-Ab_1 and fluorescent Ab_2. (e) Fluorescence image and (f) average fluorescence intensities (right) of the single peptide-modified Au surface following the CK2 kinase reactions in the absence and presence of 5 μM inhibitors: TBB, TBBz, and DMAT. Intensities were estimated from the normalized data of average intensities and error bars represent duplicate measurements.

SPR arrays are comparable to those derived from the peptide arrays on Au substrates (vide supra).

In vitro studies were performed with Hela cells at various concentrations of cell lysate in order to probe the suitability of the Fc-Ab_1 immunoassay method under dirty conditions. Up to 30% of cell lysate was added to the phosphorylation reactions using the peptide arrays. A 2-fold increase in the fluorescence intensity was observed with ~5% lysate content which was found to be an optimal value (Figure 10d). Presumably, background fluorescence becomes an issue due to the presence of numerous protein kinases which contribute to the Fc-phosphorylation reactions. Our immunoassay works in cell lysate conditions and may be used for monitoring protein phosphorylations in cellular media.

The fluorescence intensities in Figure 10e decreased when the kinase reaction was performed in the presence of 5 μM inhibitors. The fluorescence intensity in Figure 10f decreased by 75, 40, and 70% for TBB, TBBZ, and DMAT, respectively. The relative order of the inhibition is similar to that previously reported by conventional methods above. As a representative example, our immunoarray was used to estimate the IC50 value for the most potent inhibitor TBB and the estimated value of 0.5 μM was similar to that obtained by the previously reported electrochemical approach[25b] and biochemical methods based on Western blotting reported above. However, at present the fluorescence assay shows only 50% decrease in the signal in the presence of excess TBB inhibitor. The fluorescence array platform is currently being optimized for further inhibition studies. The Fc-Ab_1 methodology is amenable to inhibitor study and determination of the inhibition values.

The comparative biochemical, electrochemical, and optical studies on the Fc-phosphorylations of the target peptide or protein demonstrate that the Fc-Ab_1 assays may be used in a multiformat for detection and monitoring the biochemical processes.

■ CONCLUSIONS

We have presented the selective binding of polyclonal Fc-Ab_1 to Fc-modified biomolecules in solution and on surfaces. The methodology described was used to monitor enzymatic post-translations, such as Fc-phosphorylations, in an immunoassay format, thereby making this approach more accessible to the broader community. Results from biochemical assays and immunoarray imaging provide complementary information to the electrochemical studies and indicate the utility of the Fc-Ab_1 system in a bimodal bioanalysis. As such, the Fc-Ab_1 may likely be useful as a biosensor component for peptidomic, genomic, and pharmacogenomic analysis.

■ ASSOCIATED CONTENT

Supporting Information

Electrochemical, SPR, fluorescence imaging data, TOF-SIMS and XPS. This material is available free of charge via the Internet at http://pubs.acs.org.

■ AUTHOR INFORMATION

Corresponding Author

bernie.kraatz@utoronto.ca; litchfi@uwo.ca

Notes

The authors declare no competing financial interest.

■ ACKNOWLEDGMENTS

This research was carried out with funding from NSERC and financial support from University of Toronto Scarborough and

Western University. The authors thank G. S. Salvesen (Burnham Institute, San Diego CA).

REFERENCES

(1) (a) Hunter, T. *Cell* **2000**, *100*, 113−127. (b) Manning, G.; Whyte, D. B.; Martinez, R.; Hunter, T.; Sudarsanam, S. *Science* **2002**, *298*, 1912−1934.

(2) (a) Cohen, P. *Nat. Rev. Drug Discovery* **2002**, *1*, 309−315. (b) Flajolet, M.; He, G.; Heiman, M.; Lin, A.; Nairn, A. C.; Greengard, P. *Proc. Natl. Acad. Sci U.S.A.* **2007**, *104*, 4159−4164.

(3) Von Ahsen, O.; Bomer, U. *ChemBioChem* **2005**, *6*, 481−490.

(4) Olive, D. M. *Expert Rev. Proteomics* **2004**, *1*, 327−341.

(5) (a) Houseman, B. T.; Huh, J. H.; Kron, S. J.; Mrksich, M. *Nature* **2002**, *20*, 270−274. (b) Ptacek, J.; Devgan, G.; Michaud, G.; Zhu, H.; Zhu, X.; Fasolo, J.; Guo, H.; Jona, G.; Breitkreutz, A.; Sopko, R.; McCartney, R. R.; Schmidt, M. C.; Rachidi, N.; Lee, S. J.; Mah, A. S.; Meng, L.; Stark, M. J. R.; Stern, D. F.; De Virgilio, C.; Tyers, M.; Andrews, B.; Gerstain, M.; Schweitzer, B.; Predki, P. F.; Snyder, M. *Nature* **2005**, *438*, 679−684. (c) Zhu, H.; et al. *Nat. Genet.* **2000**, *26*, 283−289. (d) Kramer, A.; Feilner, T.; Possling, A.; Radchuk, V.; Weschke, W.; Burke, L.; Kersten, B. *Phytochemistry* **2004**, *65*, 1777−1784. (e) Schutkowski, M.; Reimer, U.; Pense, S.; Dong, L.; Lizcano, J. M.; Alessi, D. R.; Schneider-Mergner, J. *Angew. Chem., Int. Ed.* **2004**, *43*, 2671−2674.

(6) Lesaicherre, M. L.; Uttamchndani, M.; Chen, G. Y. J.; Yao, S. Q. *Bioorg. Med. Chem. Lett.* **2002**, *12*, 2085−2088.

(7) Ghadiali, J. E.; Cohen, B. E.; Stevens, M. M. *ACS Nano* **2010**, *4*, 4915−4919.

(8) Wilner, O. I.; Guidotti, C.; Wieckowska, A.; Gill, R.; Willner, I. *Chem.—Eur. J.* **2008**, *14*, 7774−7781.

(9) (a) Matsuno, H.; Furusawa, H.; Okahata, Y. *Chem.—Eur. J.* **2004**, *10*, 6172−6178. (b) Estrela, P.; Paul, D.; Li, P.; Keighley, S. D.; Migliorato, P.; Laurenson, S.; Ko Ferrigno, P. *Electrochim. Acta* **2008**, *53*, 6489−6496.

(10) Shapiro, M. G.; Szablowski, J. O.; Langer, R.; Jasanoff, A. *J. Am. Chem. Soc.* **2009**, *131*, 2484−2486.

(11) Martin, K.; Steinberg, T.; Cooley, L.; Gee, K.; Beechem, J.; Patton, W. *Proteomics* **2003**, *3*, 1244−1255.

(12) (a) Wang, Z.; Levy, R.; Fernig, D. G.; Brust, M. *J. Am. Chem. Soc.* **2006**, *128*, 2214−2215. (b) Wieckowska, A.; Li, D.; Gill, R.; Willner, I. *Chem. Commun.* **2008**, 2376−2378.

(13) (a) Hill, J. H.; Annan, R. S.; Carr, S. A.; Miller, W. T. *J. Biol. Chem.* **1994**, *269*, 7423−7428. (b) Min, D. H.; Su, J.; Mrksich, M. *Angew. Chem., Int. Ed.* **2004**, *43*, 5973−5977. (c) Green, K. D.; Pflum, M. K. H. *J. Am. Chem. Soc.* **2007**, *129*, 10−11.

(14) (a) Song, H.; Kerman, K.; Kraatz, H. B. *Chem. Commun.* **2008**, 502−504. (b) Kerman, K.; Vestergaard, N.; Tamiya, E. *Anal. Chem.* **2007**, *79*, 6881−6885.

(15) (a) Green, H. M.; Alberola-Ila, J. *BMC Chem. Biol.* **2005**, *5*, 1−8. (b) Shults, M. D.; Janes, K. A.; Lauffenburger, D. A.; Imperiali, B. *Nat. Methods* **2005**, *2*, 277−284. (c) Rhee, H. W.; Lee, S. H.; Shin, I. S.; Choi, S. J.; Park, H. H.; Han, K.; Park, T. H.; Hong, J. I. *Angew. Chem., Int. Ed.* **2010**, *49*, 4919−4923. (d) Brumbaugh, J.; Schleifenbaum, A.; Gasch, A.; Sattler, M.; Schultz, C. *J. Am. Chem. Soc.* **2006**, *128*, 24−25.

(16) (a) Elphick, L. M.; Lee, S. E.; Gouverneur, V.; Mann, D. J. *ACS Chem. Biol.* **2007**, *2*, 299−314. (b) Suwal, S.; Pflum, M. K. H. *Angew. Chem., Int. Ed.* **2010**, *49*, 1627−1630. (c) Green, K. H.; Pflum, M. K. H. *ChemBioChem.* **2009**, *10*, 234−237. (d) Allen, J. J.; Lazerwith, S. E.; Shokat, K. M. *J. Am. Chem. Soc.* **2005**, *127*, 5288−5289.

(17) (a) Gill, T. J.; Mann, L. T. *J. Immun.* **1996**, *96*, 906−912. (b) Yli-Kauhaluoma, J. T.; Ashley, J. A.; Lo, C. H.; Tucker, L.; Wolfe, M. M.; Janda, K. D. *J. Am. Chem. Soc.* **1995**, *117*, 7041−7047. (c) Heine, A.; Stura, E. A.; Yli-Kauhaluoma, J. T.; Gao, C.; Deng, Q.; Beno, B. R.; Houk, K. N.; Janda, K. D.; Wilson, I. A. *Science* **1998**, *279*, 1934−1940.

(18) Labib, M.; Shipman, P. O.; Martic, S.; Kraatz, H.-B. *Analyst* **2011**, *136*, 708−715.

(19) van Staveren, D. R.; Metzler-Nolte, N. *Chem. Rev.* **2004**, *104*, 5931−5985.

(20) (a) Duncan, J. S.; Turowec, J. P.; Duncan, K. E.; Vilk, G.; Wu, C.; Luscher, B.; Li, S. S. C.; Gloor, G. B.; Litchfield, D. W. *Sci. Signal* **2011**, *4*, 30−38. (b) Turowec, J. P.; Duncan, J. S.; French, A. C.; Gyenis, L.; St Denis, N. A.; Vilk, G.; Litchfield, D. W. *Methods Enzymol.* **2010**, *484*, 471−493.

(21) (a) Pinna, L. A. *J. Cell Sci.* **2002**, *115*, 3873−3878. (b) Duncan, J. S.; Turowec, J. P.; Vilk, G.; Li, S. S.; Gloor, G. B.; Litchfield, D. W. *Biochim. Biophys. Acta* **2010**, *1804*, 505−510.

(22) Sarno, S.; Ghisellini, P.; Pinna, L. A. *J. Biol. Chem.* **2002**, *277*, 22509−22514.

(23) (a) Fischer, E. H.; Krebs, E. G. *J. Biol. Chem.* **1995**, *216*, 121−132. (b) Malumbres, N.; Barbacid, M. *Nat. Rev* **2009**, *9*, 153−166. (c) Litchfield, D. W. *Biochem. J.* **2003**, *369*, 1−15. (d) Wu, K. J.; Mattiolo, M.; Morse, H. C.; Dalla-Favera, R. *Oncogene* **2002**, *21*, 7872−7882.

(24) Martic, S.; Rains, M. K.; Freeman, D.; Kraatz, H. B. *Bioconjugate Chem.* **2011**, *22*, 1663−1672.

(25) (a) Martic, S.; Beheshti, S.; Rains, M. K.; Kraatz, H.-B. *Analyst* **2012**, *137*, 2042−2046. (b) Kerman, K.; Song, H.; Duncan, J. S.; Litchfield, D. W.; Kraatz, H.-B. *Anal. Chem.* **2008**, *80*, 9395−9401.

(26) Chen, J.; Winograd, N. *Anal. Chem.* **2005**, *77*, 3651−3659.

(27) (a) Ladd, J.; Zhang, Z.; Chen, S.; Hower, J. C.; Jiang, S. *Biomacromolecules* **2008**, *9*, 1357−1361. (b) Ray, S.; Shard, A. G. *Anal. Chem.* **2011**, *83*, 8659−8666.

(28) Neff, P. A.; Serr, A. *ChemPhyChem* **2007**, *8*, 2133−2137.

(29) (a) Rich, R. L.; Myszka, D. G. *Curr. Opin. Biotechnol.* **2000**, *11*, 54−61. (b) Nelson, B. P.; Frutos, A. G.; Brockman, J. M.; Corn, R. M. *Anal. Chem.* **1999**, *71*, 3928−3934. (c) Brockman, J. M.; Merlson, B. P.; Cron, R. M. *Annu. Rev. Phys. Chem.* **2000**, *51*, 41−63.

(30) (a) Takeda, H.; Fukumoto, A.; Miura, A.; Goshina, N.; Nomura, N. *Anal. Biochem.* **2006**, *357*, 262−271. (b) Li, J.; Smith, G. P.; Walker, J. C. *Proc. Natl. Acad. Sci. U.S.A.* **1999**, *96*, 7821−7826. (c) Inamori, K.; Kyo, M.; Nishiya, Y.; Inoue, Y.; Sonoda, T.; Kinoshita, E.; Koike, T.; Katayama, Y. *Anal. Chem.* **2005**, *77*, 3979−3985.

(31) Marengere, L. E. M.; Songyang, Z.; Gish, G. D.; Schaller, M. D.; Parson, J. T.; Stern, M. J.; Cantley, L. C.; Pawson, T. *Nature* **1994**, *369*, 502−505.